Gas-Phase Spectroscopy of Protonated 3-OH Kynurenine and Argpyrimidine. Comparison of Experimental Results to Theoretical Modeling

Line Kessel,*,† Iben B. Nielsen,‡ Anastasia V. Bochenkova,§ Ksenia B. Bravaya,§ and Lars H. Andersen‡

Department of Ophthalmology, Glostrup Hospital, University of Copenhagen, Denmark, Department of Physics and Astronomy, University of Aarhus, Denmark, and Department of Chemistry, Moscow State University, Russian Federation

Received: June 8, 2007; In Final Form: August 21, 2007

The aging process of the human lens is associated with accumulation of chromophores and fluorophores that impair visual function. In the present study, we examined the photodissociation of 3-OH-kynurenine and argpyrimidine. Furthermore, absorption spectra obtained in gas phase using an electrostatic ion storage ring were studied as gas phase absorption have been shown to be more similar to the in vivo condition than absorption spectra obtained in the liquid phase. Experimental results were compared to theoretical modeling using the multistate, multireference perturbation theory approach combined with advanced molecular modeling tools to account for the solvent effects and to provide direct support for band assignments. Absorption maxima were determined both experimentally and theoretically and significant differences between the two chromophores were found. In particular, 3-OH-kynurenine demonstrated a blue-shift of more than 130 nm in the aqueous phase compared to the gas-phase due to the existence of different 3-OH-kynurenine conformers, which are stable under different conditions and originate from the interplay between intra- and intermolecular interactions. Photodissociation of argpyrimidine and 3-OH-kynurenine was observed in vacuum thus confirming the results previously obtained in liquid phase demonstrating that the photodestruction takes place in both media.

Introduction

As the human lens ages, several physical changes are observed, most notably an increased yellow-brownish coloration that is accompanied by an increase in autofluorescence.[1,2] The lens is unique from most other tissues in that there is no removal of damaged cell organelles or proteins. In the long term, the age-related changes impair visual function by increasing absorption and scattering, a condition which is termed cataract. Eventually, it will lead to blindness if not treated. A large number of chromophores and fluorophores have been identified falling into two major groups: posttranslational protein modification by glucose through formation of advanced glycation end products[3−6] and tryptophan metabolites such as the kynurenines.[7−10]

The role of the chromophores is dual. In the young lens, the chromophores absorb light thus protecting the retina from damage by ultraviolet radiation. However, some of the chromophores may also function as photosensitizers,[11] which as their concentration increases with age, hypothetically, could accelerate photochemical reactions in the lens, thus leading to further damage.

A great number of studies have been carried out to characterize the properties of the chromophores and fluorophores related to the aging process in the lens. These studies have, however, all been carried out on chromophores or fluorophores in liquids, mainly aqueous solutions. Changes in local environment are known to have a major impact on absorption and fluorescence properties due to hydrogen bonding, dipole moments, changes in pH, etc.,[12] and spectra may shift more than 100 nm due to solvent changes.[13] Unfortunately, very little is known about the local microenvironment of the fluorophores and chromophores in the lens.

In the present work, we have investigated the absorption properties of the isolated chromophores in vacuo, and our work may serve as a reference representing the zero-perturbation case where the chromophore is in an environment devoid of external perturbations such as external charges and dipoles. More specifically, we used gas-phase spectroscopy to study absorption and photodissociation of 3-OH-kynurenine and argpyrimidine. Both are well-characterized chromophores that have been implicated in the aging process of the human lens.[5,7] Furthermore, we carried out an extensive ab initio study on their photoabsorption spectra in the gas phase and solution to give an insight into the possible role played by local environments. The key questions addressed in the theoretical part of the present study are the sensitivity of excitation energies to changes in the microenvironment and factors contributing to solvent shifts.

Studies on photoactive proteins like the green fluorescent protein (GFP) have demonstrated that gas-phase spectroscopy has the advantage over solution-phase spectroscopy because the spectra obtained may be closer to the native condition with the chromophore in situ in the intact protein.[14−17] In the gas phase, the molecules are studied without influence of external dipole moments, intermolecular hydrogen bonding, or other effects that may affect absorption and fluorescence. The conditions in certain proteins like GFP resemble those of a vacuum because the

* To whom correspondence should be addressed. Phone: +45 43 23 23 00. Fax: +45 43 23 46 69. E-mail: line.kessel@dadlnet.dk.
† University of Copenhagen.
‡ University of Aarhus.
§ Moscow State University.

10.1021/jp074441h CCC: $37.00
Published on Web 10/03/2007

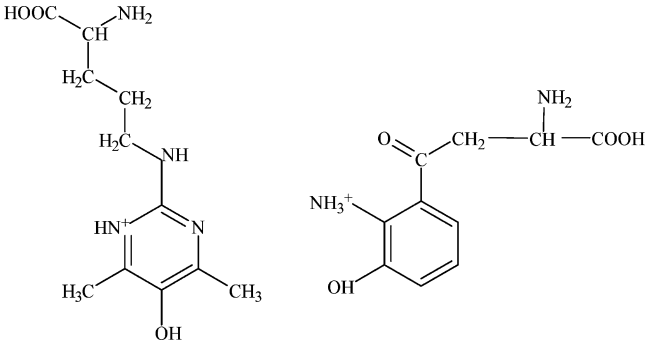

Figure 1. A schematic drawing of the two chromophores studied in the present work. Left, argpyrimidine (m = 255 amu); right, 3-OH-kynurenine (m = 225 amu).

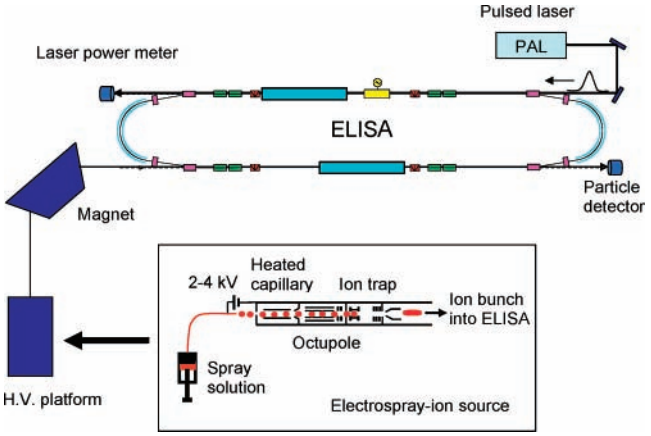

Figure 2. The ELISA storage ring with the electrospray ion source shown in the insert.

chromophore is placed in an isolated protein pocket where there is very little exposure to water. Indeed, it is often a bad choice to use liquid-phase measurements as a reference for the absorption spectrum of isolated biochromophores as will be demonstrated in the present work.

Experimental Methods

Experimental Details. In the present study, two chromophores were considered, 3-OH-kynurenine and argpyrimidine. 3-OH-kynurenine is a tryptophan metabolite that absorbs ultraviolet radiation, thus protecting the retina from damage by ultraviolet radiation. Argpyrimidine is a posttranslational protein modification formed by a reaction by methylglyoxal and arginine.[5] 3-OH-kynurenine was purchased from Sigma-Aldrich (Sigma-Aldrich, Vallensbæk, Denmark). Argpyrimidine was kindly provided by Dr. R.H. Nagaraj, Department of Ophthalmology, Case Western Reserve University, Cleveland, Ohio. 3-OH-kynurenine is the only one of the kynurenine derivates commercially available and was chosen for this reason even though it is not the most abundant in the human lens.[18] The two chromophores considered in the present study are shown schematically in Figure 1. For gas-phase spectroscopy, the chromophores were protonated and hence cations.

To study the absorption characteristics of the two chromophores in the gas-phase we used the electrostatic ion storage ring in Aarhus, Denmark, (ELISA)[19,20] (Figure 2). The chromophore molecules are first electronically excited by light from a pulsed laser. The internal energy is quickly converted into nuclear vibrations (internal conversion) and as a result fragmentation may occur, typically on the submillisecond time scale. The storage ring technique is essential to the work, because it allows us to record the delayed action (dissociation) of the photoexcitation of the chromophore.

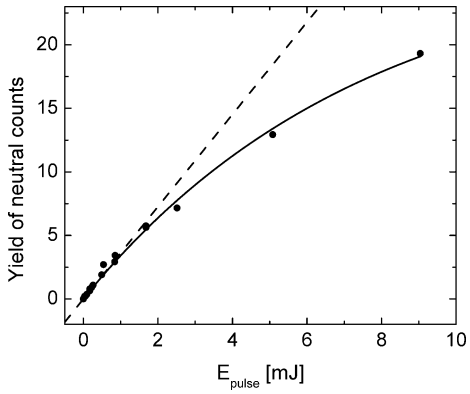

Figure 3. Yield of neutrals for 3-OH-kynurenine as a function of the laser pulse energy (λ = 450 nm).

Freshly prepared chromophore samples were brought into the gas phase by an electrospray-ion source.[21] The ions are accumulated for 100 ms in an ion trap with a helium buffer gas, which cools them down to room temperature. After extraction and acceleration to a kinetic energy of 22 keV, the desired ions are selected by a bending magnet, and about 10 μs long bunches of typically 10^4 ions are injected into the storage ring at a repetition rate of 10 Hz. The ions circulate in the ring with a revolution time of about 60 μs until they change their mass-to-charge ratio either by unimolecular dissociation or by collisions with residual gas (pressure $\sim 10^{-11}$ mbar). Neutral particles are not deflected by the electric fields in ELISA and continue on straight trajectories. Those formed in the first section of the ring hit a microchannel plate detector located at the end of this section (see Figure 2) and constitute the signal of absorption.

The chromophore ions are irradiated after about 60 milliseconds of storage. The tunable, visible laser light is provided by an Alexandrite laser (101 PAL laser, Light Age) together with a Raman scattering cell (30 ns pulse duration). Laser pulse energy was in the order of 0.1−1 mJ throughout the 300−600 nm region. Tuning of the laser wavelength to an absorption band results in bond dissociation and hence in the formation of detectable neutral products. Data are accumulated in steps of about 5 nm with typically one thousand injections at each wavelength.

The laser excitation causes a significant increase in the count rate of neutral photo fragments. The signal is due to dissociation caused by the $\sim$3 eV increase in internal energy ($\lambda \sim$ 400 nm). Briefly, we start with the chromophore in the electronic ground state at room temperature where only a few of the $3N - 6$ vibrational modes are excited (N is the number of atoms in the molecule). Photoabsorption brings the molecule into the first excited state, and radiationless internal conversion[22] brings the molecule back to the electronic ground state with about 2−4 eV of energy distributed over the vibrational modes. This eventually leads to dissociation on the submillisecond time scale. Such decays have been modeled successfully with an Arrhenius expression for the decay rate.[22,23]

Figure 3 shows the yield of neutrals for 3-OH-kynurenine as a function of the laser-pulse energy. Initially, a linear effect is noted, which flattens off at laser-pulse energies in excess of 2 mJ. This shows that at the present wavelengths only one photon is required to dissociate the chromophore. The deviation from a linear behavior is ascribed to multiple photon absorption

within the laser pulse of several nanoseconds duration. The increasing internal energy associated with multiphoton absorption leads to very fast fragmentation that will not be seen by the present detector located at the side of ELISA opposite to the laser interaction region; hence, we observe less neutral counts at the higher laser-pulse energy. Saturation also results from the finite number of ions in the laser path.

From the measured power dependence of the yield, the photodissociation process was found to proceed through one-photon absorption at low laser-powers, and the photoabsorption cross section $\sigma(\lambda)$ is hence given as

$$\sigma(\lambda) \propto \frac{N(\lambda) - N_0}{N_0} / \frac{<E_{\text{pulse}}>}{hc/\lambda} \qquad (1)$$

where $N(\lambda)$ is the total counts of neutral particles in the signal peak. N_0 is a small contribution of neutrals from residual gas collisions, which is subtracted. N_0 is proportional to the number of ions in the ring and is therefore used for normalization. $<E_{\text{pulse}}>$ is the average laser-pulse energy, and $<E_{\text{pulse}}>/(hc/\lambda)$ is the number of photons in the laser pulse at wavelength λ. We do not know the exact overlap between the ion beam and the laser beam and hence do not obtain absolute cross sections.

A GBC 920 spectrophotometer (GBC, Inc., Australia) was used for absorption measurements of argpyrimidine and 3-OH-kynurenine in the aqueous phase.

Computational Details. The equilibrium geometry parameters for the ground state of 3-OH-kynurenine and argpyrimidine in the gas phase were determined using density functional theory (DFT) in conjunction with PBE0 hybrid functional. The correlation consistent cc-pVDZ basis set augmented with diffuse functions on the oxygen and nitrogen atoms was employed throughout the present study.

Vertical excitation energies were calculated in the frame of the augmented effective Hamiltonian technique based on the second-order multiconfigurational quasi-degenerate perturbation theory (MCQDPT2). Initially, the reference wavefunctions of the low-lying singlet states were obtained through state-averaged complete active space self-consistent field (CASSCF) calculations. The active spaces comprised a complete set of π-orbitals spanned over the entire conjugated system for all species. They were further extended to include the lone-pair orbitals of the ring nitrogen atoms of argpyrimidine and the oxygen atom of the carbonyl bond of 3-OH-kynurenine. In particular, the active spaces included (12 electrons/9 orbitals) and (14/10) for protonated and neutral argpyrimidine, and (12/10) and (14/11) for protonated and neutral 3-OH-kynurenine, respectively.

The reference CASSCF wavefunctions were used in a subsequent multistate multireference perturbation theory (MRPT) calculation based on the MCQDPT2 formalism accounting for dynamic electron correlation effects.[24] In addition, the reference zeroth-order states were allowed to interact under the influence of dynamic correlation through the effective Hamiltonian calculated perturbatively. The states of interest were obtained simultaneously by the diagonalization of the effective Hamiltonian within the chosen reference space and were based on linear combinations of the CASSCF wavefunctions. The reference spaces used for the perturbative treatment were spanned by up to 15 CASSCF roots. Sequentially enlarged dimensions of the model space were used to construct a series of augmented effective Hamiltonians to guarantee a stable saturated electronic solution for the target low-lying excited states. To avoid high-energy intruder states to be coupled with the target valence wavefunction, the intruder state avoidance technique was applied.[25] Furthermore, the quality of each additional zeroth-order state was tested before diagonalization of the effective Hamiltonian. The accidental states were identified and excluded from the extended MCQDPT2 calculations by estimating the norm of their projections on the secondary space.

In the present study, we extended the applicability of the augmented effective Hamiltonian technique to model excitation energies of the two biological chromophores in solution. The strategy used here has two major steps: the ground-state geometry optimization with an explicit solvation model and evaluation of transition energies of chromophores treated at the augmented MCQDPT2 level in the external electrostatic field originated from the distributed multipoles of water molecules.

Initial geometry configurations of the chromophores embedded in a cluster of around 200 water molecules was prepared in the following way. According to the pKa values of the functional groups of the alpha-aminoacids in water solutions, we considered the zwitterionic aminoacid species in all calculations performed in water surroundings. Each chromophore molecule was uniformly solvated by water molecules followed by thermal equilibration of the environment at 298 K during 20 ps and gradual relaxation to 0 K during the same time interval by using the molecular dynamics technique with the standard CHARMM[26] force-field parameters. The molecular modeling package TINKER (J. W. Ponder, http://dasher.wustl.edu/tinker) was utilized in these molecular dynamics simulations. Equilibrium geometry configurations of the entire molecular systems were further optimized by using the combined quantum mechanical−effective fragment potential (EFP) technique[27] as originally implemented by M.S. Gordon et al. within the GAMESS computational package.[28] The EFP approach was specifically developed to model solvent effects in polar solutions with strong hydrogen-bonding interactions. Chromophore molecules were treated at the same quantum mechanical level of theory as gas-phase species. Each water molecule was replaced by an effective fragment. The effective fragment potentials incorporated the most important nonbonded interaction energy terms: Coulomb interaction, self-consistent polarization, and exchange repulsion. All terms were included as one-electron contributions to the quantum mechanical Hamiltonian of the chromophore molecule. The EFP parameters included distributed multipole expansion points, consisting of charges through octupoles located at all atomic centers and bond midpoints, dipole polarizability tensors, and repulsive points. We used standard parameters for the water molecules, which were previously calculated and fitted in separate ab initio runs.

Through the use of entirely optimized geometries of the molecular systems, the excitation energies were computed by the combined augmented MCQDPT2 technique and the EFP approach. Here, only the main contributions from effective fragment potentials were taken into account. In particular, distributed partial charges, dipoles, quadrupoles, and octupoles were considered at this stage. The combined methodology applied in this work incorporates both an impact of water molecules on the equilibrium geometry configuration of the central part through the major charge−dipole and hydrogen-bonding interactions and electronic effects allowing for polarization of the ground- and excited-state electron densities by external environmental field.

An efficient implementation of the augmented MCQDPT2 approach and parallel versions of DFT, CASSCF, and EFP methods were used as a part of the PC GAMESS quantum chemistry package (A.A. Granovsky, http://lcc.chem.msu.ru/gran/gamess/index.html).

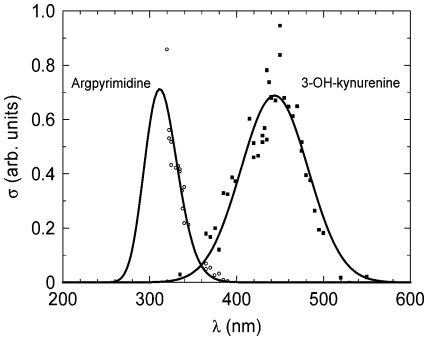

Figure 4. The absorption cross section of protonated argpyrimidine (open circles, left curve) and protonated 3-OH-kynurenine (bold squares, right curve) recorded in the gas phase. The 3-OH-kynurenine data were fitted with a Gaussian function yielding a maximum at 444 nm. The argpyrimidine data were fitted with a Gaussian of the same energy width as that obtained in the fit to the 3-OH-kynurenine data yielding a maximum of absorption at 310 nm.

Results

3-OH-Kynurenine. The gas phase absorption spectrum of 3-OH-kynurenine cations is shown in Figure 4. It shows a maximum of absorption at 444 ± 5 nm. The absorption characteristics are found to be highly dependent on changes in the local environment as the maximum is blue-shifted by more than 130 nm in acidic water (Table 1).

The lowest-energy equilibrium geometry configurations of the gas-phase 3-OH-kynurenine cation and its neutral form are presented in Figure 5. The optimized structures reveal the existence of intramolecular hydrogen-bonding interactions in both cases. The protonated form is characterized by the positive charge located at the amino group of the ring. The strong interaction of this positive charge with the most electrodonor acid functional group of 3-OH-kynurenine dictates a highly twisted conformation of the chromophore in the gas phase. It leads to partial breaking of the conjugated π-system with the O═C−C═C angle being equal to 39°. In the neutral form where the intramolecular interactions are not so strong, the π-conjugation restores, being energetically more favorable over the twisted conformation. In addition, the lone pair of the amino group actively participates in the π-conjugation.

From the above consideration, we may expect an interplay between two factors that determine the equilibrium geometry configuration of 3-OH-kynurenine in solution: intramolecular interactions including hydrogen bonding and π-conjugation, and intermolecular interactions of the chromophore with water molecules. Changes in excitation energies observed in solutions characterized by different pH values can be unambiguously traced to different protonation states of the functional groups in the chromophore. Thus, neutral molecules and protonated forms embedded in a water cluster are considered to model neutral and acidic conditions, respectively. The possible influence of a counterion in acidic solutions is neglected in the present study, because we expect an effective shielding of the counterion by water molecules.

A number of nearly equal probable minima on the potential energy surface (regarding their energy) were located for the neutral and protonated molecules embedded in water clusters. They differ by orientation of the aminoacid zwitterionic tail with respect to the π-conjugated part of the molecule. As an example, one of the possible equilibrium geometries of the neutral and protonated forms of 3-OH-kynurenine in water solution is presented in Figure 6. Because 3-OH-kynurenine chromophore has very short distance between aminoacid zwitterion and the ring, different orientations of its highly polarized tail may contribute to some deviations in excitation energies depending on the particular geometry. Two limiting cases with respect to the torsional angle around the $C_\alpha-C_\beta$ bond were considered at the second stage. According to the results obtained, the neutral form preserves the planar structure. The protonated 3-OH-kynurenine is stabilized by water molecules and, as a result, almost restores the planarity of the conjugated system.

Because the equilibrium geometries in the gas phase of the 3-OH-kynurenine cation and its neutral forms are qualitatively different, we might expect pronounced deviations in their excitation energies. The results obtained through the augmented MCQDPT2 technique coupled with the EFP approach are presented in Table 1. The theoretical results agree well with the experimental photoabsorption maxima, though several precautions apply when comparing experiment with theory. The full width of the band at half-maximum assumes identical vibrational excitations, thus introducing some uncertainty in the definition of the experimental pure electronic S_0-S_1 transition.

The nature of the low-lying excited states of the different forms of 3-OH-kynurenine relates to both $\pi-\pi^*$ and $n-\pi^*$ transitions. The first exited state has $\pi-\pi^*$ character, but the order of states drastically depends on the level of theory. In particular, the target state is only the third root at both CASSCF and second-order multireference Møller−Plesset perturbation theory (MRMP2) levels in the case of 3-OH-kynurenine cation. The augmented effective Hamiltonian technique applied in the present study corrects the deficiencies of CASSCF reference wavefunction, providing the correct ordering of states and leading to the localization of the wavefunction in terms of its expansion through the configurational state functions.

It is worth to note that the smallest S_0-S_1 energy gap corresponds to the protonated form of 3-OH-kynurenine in the gas phase (452 nm). The nonplanarity leads to the partial breaking of the conjugated π-system. Reduction of the delocalized electron systems usually results in a blue shift when the transition occurs in the frame of one π-system. In the case of 3-OH-kynurenine cation, the electronic transition is accompanied by the electron density redistribution from the conjugated ring to the carbonyl group. As a result, two π-systems interact through the excitation. The character of the first excited-state is illustrated in terms of natural CASSCF orbitals mainly involved in the transition (see Figure 7). This $\pi-\pi^*$ configurational state function has a leading coefficient of 0.83 in the expansion of the target wavefunction after diagonalization of the effective Hamiltonian accounting for dynamic electron correlation effects.

The excitation energy of the neutral gas-phase molecule undergoes a blue shift and is equal to 379 nm. The environment does not appear to have much influence on the energy gap of the planar neutral 3-OH-kynurenine. Because the equilibrium structures and the character of the S_0-S_1 electronic transition

TABLE 1: Absorption Maxima of the Two Chromophores in the Gas Phase and in Water Solution

		gas phase	water, neutral	water, acidic	water, alkaline
3-OH-kynurenine	experiment	444 ± 5 nm	365−375	310−320	390−400
	theory	452 nm	368, 379	328	
argpyrimidine	experiment	<320 nm	325−330	335−340	335−340
	theory	319 nm	320	338	

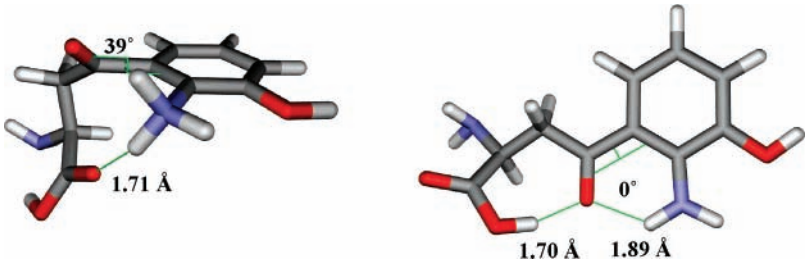

Figure 5. Lowest-energy structures for the gas-phase 3-OH-kynurenine. Left, protonated form; right, neutral form.

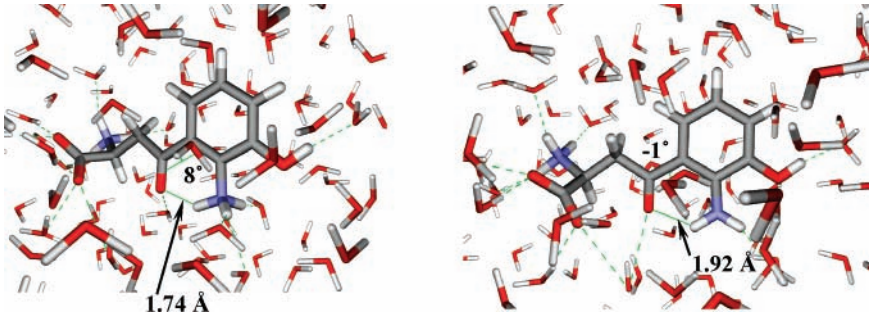

Figure 6. Equilibrium geometry configurations of 3-OH-kynurenine in water solutions. Left, protonated form in acidic solution; right, neutral form in neutral solution.

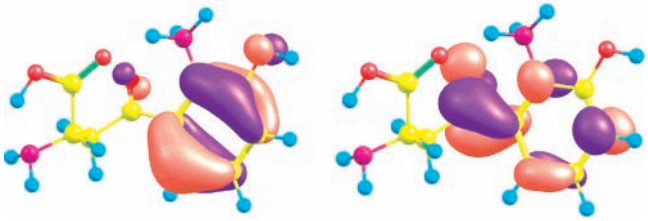

Figure 7. Natural CASSCF orbitals involved in the S_0-S_1 transition in the protonated form of 3-OH-kynurenine in the gas phase.

in the neutral 3-OH-kynurenine in the gas phase and solution are similar, it is reasonable to expect an equal energy stabilization for the ground and first excited states. The two values 379 and 368 nm correspond to the equilibrium geometry configurations differing by the torsion angle around $C_\alpha-C_\beta$ bond (angle $(H_3)N-C-C-C(=O)$), being equal to 50 and $-153°$, respectively. They give an estimation of the possible broadening of the band, which equals approximately 10 nm. The nearly planar protonated form of 3-OH-kynurenine in solution, which resembles the structure of the neutral form, exhibits an additional blue shift caused by a preferential energy stabilization of the ground state by the environment.

Argpyrimidine. Maximum absorption of argpyrimidine in the gas phase was found to be below 320 nm (Figure 4). Unfortunately, we do not have tuneable laser light available below 320 nm. To give our best estimate to the peak position, we used a Gaussian fit to the partially measured absorption profile with the same energy width as that of the absorption curve of the 3-OH-kynurenine data. The absorption of argpyrimidine in an aqueous solution is found to be rather insensitive to the state of protonation because absorption in water solutions of different pH values gives almost identical absorption maxima. Compared to the maximum in vacuum, we can only state that acidic as well as alkaline water red shift the absorption (Table 1) but perhaps not by very much. The measured power dependence of the absorption signal at $\lambda = 325$ nm only showed very little deviation from a linear behavior. Because of limitations of the laser power at the short wavelengths, which had to be used for this chromophore, we only studied the power dependence in the low power region ($E_{pulse} < 0.3$ mJ).

The calculated equilibrium geometry configurations of the protonated and neutral forms of argpyrimidine in the gas phase and solution are presented in Figure 8. The optimized structures of the protonated and neutral forms are quite similar. Certain deviations in torsional angles reflect a slightly different conjugation with the π-lone pair of the nonring nitrogen atom being effectively involved in the delocalization by the positive charge of the ring in the case of cation. Theoretical estimates for the S_0-S_1 energy gap obtained through the augmented MCQDPT2 technique coupled with the EFP approach are presented in Table 1. The nature of the first excited state refers to the $\pi-\pi^*$ transition as in the case of 3-OH-kynurenine. The S_0-S_1 excitation energies for the protonated and neutral argpyrimidine in the gas phase are close to each other, being equal to 319 and 306 nm, respectively. Furthermore, environmental effects are nearly negligible in the case of argpyrimidine. The similarity in the equilibrium structures with respect to the π-conjugation and an equal energy stabilization of the ground and first excited states by the environment leads to almost identical excitation energies of the different argpyrimidine forms.

Discussion

The aging process of the lens has been widely studied, and a number of chromophores and fluorophores have been identified. The aim of the present work was to study representatives of two major groups of chromophores in the lens in the gas phase. We studied absorption characteristics and photodissociation. The argpyrimidine absorption spectra in the gas phase were very similar to those obtained in water[12] so the absorption characteristics of argpyrimidine were largely preserved even in case of major changes in the local environment. The tryptophan metabolite, 3-OH-kynurenine, however demonstrated very large variations in the absorption spectrum obtained in the gas phase compared to those obtained in the aqueous phase, and absorption characteristics of 3-OH-kynurenine were found to be highly dependent on the local environment. On the basis of advanced calculations, such different behaviors were traced to the existence of different 3-OH-kynurenine conformers, which are stable under different conditions and originated from the interplay between intra- and intermolecular interactions.

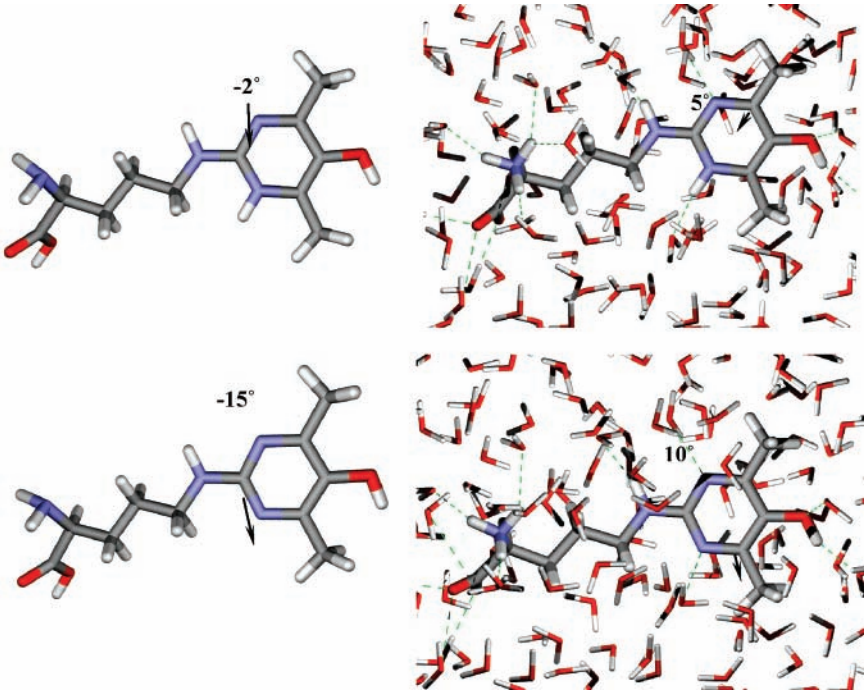

Figure 8. Equilibrium geometry configurations of argpyrimidine. Upper panel: protonated form in the gas phase (left) and in acidic solution (right). Lower panel: neutral form in the gas phase (left) and in the neutral solution (right).

The local microenvironment of the various chromophores and fluorophores in situ in the lens is unknown. Most in vivo studies on lens fluorescence have been carried out using the Fluorotron (Ocumetrics, San Jose, CA), which excites at 430−490 nm and detects fluorescence at 530−630 nm. Very few fluorophores absorbing and emitting in this range have been described based on in vitro studies.[29] We found that the fluorescence of 3-OH-kynurenine may shift up to 130 nm depending on changes in the local environment. The fluorescence observed in vivo may thus be very different from that observed in vitro and reference from in vitro studies to the in vivo situation should only be drawn with precautions.

The tryptophan metabolite 3-OH-kynurenine was found to be susceptible to photodissociation in the gas phase. Previously, we found that 3-OH-kynurenine showed significant reduction in absorption after exposure to strong UVR-A in aqueous solution.[30] The role of kynurenine in the aging process of the lens is complex. It has been stated that the role of 3-OH-kynurenine is antioxidative[31] thus protecting the lens from oxidative damage mainly from ultraviolet radiation through transferring energy of the incoming ultraviolet radiation to species that are too short lived to transfer energy to other molecules.[32] It does seem, however, that 3-OH-kynurenine itself is destructed by UVR-A; this along with the conversion of 3-OH-kynurenine to xanthurenic acid[33] may explain the reduced content of 3-OH-kynurenine with age.[18] Hypothetically, this could make the lens more susceptible to photochemical destruction as the individual ages thus accelerating the rate of the aging processes in the senescence.

In conclusion, the present study demonstrated that the spectral characteristics of 3-OH-kynurenine were highly influenced by changes in the local environment whereas those of argpyrimidine seemed largely unaffected. This finding is fully consistent with the theoretical calculations presented in this work. 3-OH-kynurenine and argpyrimidine were found to be susceptible to one-photon photochemical destruction, which may be of significance for the aging process of the lens in vivo.

Acknowledgment. The authors are grateful to Dr. R. H. Nagaraj, Department of Ophthalmology, Case Western Reserve University, Cleveland, Ohio, for providing the argpyrimidine used in the present work. The study received financial support from The Danish Medical Research Council (Grant 721-05-0689), The Danish National Advanced Technology Foundation, the Lundbeck and Velux Foundations, and the Danish Natural Science Research Council (Grant 272-06-0427). A.V.B. and K.B.B. also thank Russian Science Support Foundation and Russian Foundation for Basic Research (Grant 07-03-00059) for financial support.

References and Notes

(1) Bron, A. J.; Vrensen, G. F.; Koretz, J.; Maraini, G.; Harding, J. J. The aging lens. *Ophthalmologica* **2000**, *214*, 86−104.

(2) Lerman, S.; Borkman, R. Spectroscopic evaluation and classification of the normal, aging, and cataractous lens. *Ophthalmic Res.* **1976**, *8*, 335−353.

(3) Monnier, V. M.; Cerami, A. Nonenzymatic browning in vivo: possible process for aging of long-lived proteins. *Science* **1981**, *211*, 491−493.

(4) Tessier, F.; Obrenovich, M.; Monnier, V. M. Structure and mechanism of formation of human lens fluorophore LM-1. Relationship to vesperlysine A and the advanced Maillard reaction in aging, diabetes, and cataractogenesis. *J. Biol. Chem.* **1999**, *274*, 20796−20804.

(5) Padayatti, P. S.; Ng, A. S.; Uchida, K.; Glomb, M. A.; Nagaraj, R. H. Argpyrimidine, a blue fluorophore in human lens proteins: high levels in brunescent cataractous lenses. *Invest. Ophthalmol. Visual Sci.* **2001**, *42*, 1299−1304.

(6) Ulrich, P.; Cerami, A. Protein glycation, diabetes, and aging. *Recent Prog. Horm. Res.* **2001**, *56*, 1−21.

(7) Pirie, A. Formation of N′-formylkynurenine in proteins from lens and other sources by exposure to sunlight. *Biochem. J.* **1971**, *125*, 203−208.

(8) Ellozy, A. R.; Wang, R. H.; Dillon, J. Model studies on the photochemical production of lenticular fluorophores. *Photochem. Photobiol.* **1994**, *59*, 479−484.

(9) Roberts, J. E.; Finley, E. L.; Patat, S. A.; Schey, K. L. Photooxidation of lens proteins with xanthurenic acid: a putative chromophore for cataractogenesis. *Photochem. Photobiol.* **2001**, *74*, 740−744.

(10) Davies, M. J.; Truscott, R. J. Photo-oxidation of proteins and its role in cataractogenesis. *J. Photochem. Photobiol., B* **2001**, *63*, 114−125.

(11) Roberts, J. E. Ocular phototoxicity. *J. Photochem. Photobiol., B* **2001**, *64*, 136−143.

(12) Kessel, L.; Kalinin, S.; Nagaraj, R. H.; Larsen, M.; Johansson, B-Å. L. Time-resolved and steady-state fluorescence spectroscopic studies of the human lens with comparison to argpyrimidine, pentosidine and 3-OH-kynurenine. *Photochem. Photobiol.* **2002**, *76*, 549−554.

(13) Lakowicz, J. R. *Principles of Fluorescence Spectroscopy*; Kluwer Academic/Plenum Publishers: New York, 1999.

(14) Andersen, L. H.; Lapierre, A.; Nielsen, S. B.; Nielsen, I. B.; Pedersen, S. U.; Pedersen, U. V.; Tomita, S. Chromophores of the green fluorescent protein studied in the gas phase. *Eur. Phys. J. D* **2002**, *20*, 597−600.

(15) Boyé, S.; Nielsen, S. B.; Krogh, H.; Nielsen, I. B.; Pedersen, U. V.; Bell, A. F.; He, X.; Tonge, P. J.; Andersen, L. H. Gas-phase absorption properties of DsRed model chromophores. *Phys. Chem. Chem. Phys.* **2003**, *5*, 3021−3026.

(16) Nielsen, I. B.; Boye-Peronne, S.; El Ghazaly, M. O. A.; Kristensen, M. B.; Nielsen, S. B.; Andersen, L. H. Absorption spectra of photoactive yellow protein chromophores in vacuum. *Biophys. J.* **2005**, *89*, 2597−2604.

(17) Nielsen, S. B.; Lapierre, A.; Andersen, J. U.; Pedersen, U. V.; Tomita, S.; Andersen, L. H. Absorption spectrum of the green fluorescent protein chromophore anion in vacuo. *Phys. Rev. Lett.* **2001**, *87*, 228102.

(18) Bova, L. M.; Sweeney, M. H.; Jamie, J. F.; Truscott, R. J. Major changes in human ocular UV protection with age. *Invest. Ophthalmol. Vis. Sci.* **2001**, *42*, 200−205.

(19) Andersen, L. H.; Heber, O.; Zajfman, D. Physics with electrostatic rings and traps. *J. Phys. B: At. Mol. Opt. Phys.* **2004**, *37*, R57−R88.

(20) Møller, S. P. ELISA, an electrostatic storage ring for atomic physics. *Nucl. Instrum. Methods Phys. Res., Sect. A* **1997**, *394*, 281−286.

(21) Andersen, J. U.; Hvelplund, P.; Nielsen, S. B.; Tomita, S.; Wahlgreen, H.; Moller, S. P.; Pedersen, U. V.; Forster, J. S.; Jorgensen, T. J. D. The combination of an electrospray ion source and an electrostatic storage ring for lifetime and spectroscopy experiments on biomolecules. *Rev. Sci. Instrum.* **2002**, *73*, 1284−1287.

(22) Andersen, L. H.; Bluhme, H.; Boye, S.; Jorgensen, T. J. D.; Krogh, H.; Nielsen, I. B.; Nielsen, S. B.; Svendsen, A. Experimental studies of the photophysics of gas-phase fluorescent protein chromophores. *Phys. Chem. Chem. Phys.* **2004**, *6*, 2617−2627.

(23) Nielsen, S. B.; Andersen, J. U.; Forster, J. S.; Hvelplund, P.; Liu, B.; Pedersen, U. V.; Tomita, S. Photodestruction of adenosine 5′-monophosphate (AMP) nucleotide ions in vacuo: Statistical versus non-statistical processes. *Phys. Rev. Lett.* **2003**, 91.

(24) Nakano, H. Quasi-Degenerate Perturbation-Theory with Multiconfigurational Self-Consistent-Field Reference Functions. *J. Chem. Phys.* **1993**, *99*, 7983−7992.

(25) Witek, H. A.; Choe, Y. K.; Finley, J. P.; Hirao, K. Intruder state avoidance multireference Moller-Plesset perturbation theory. *J. Comput. Chem.* **2002**, *23*, 957−965.

(26) MacKerell, A. D.; Bashford, D.; Bellott, M.; Dunbrack, R. L.; Evanseck, J. D.; Field, M. J.; Fischer, S.; Gao, J.; Guo, H.; Ha, S.; Joseph-McCarthy, D.; Kuchnir, L.; Kuczera, K.; Lau, F. T. K.; Mattos, C.; Michnick, S.; Ngo, T.; Nguyen, D. T.; Prodhom, B.; Reiher, W. E.; Roux, B.; Schlenkrich, M.; Smith, J. C.; Stote, R.; Straub, J.; Watanabe, M.; Wiorkiewicz-Kuczera, J.; Yin, D.; Karplus, M. All-atom empirical potential for molecular modeling and dynamics studies of proteins. *J. Phys. Chem. B* **1998**, *102*, 3586−3616.

(27) Gordon, M. S.; Freitag, M. A.; Bandyopadhyay, P.; Jensen, J. H.; Kairys, V.; Stevens, W. J. The effective fragment potential method: A QM-based MM approach to modeling environmental effects in chemistry. *J. Phys. Chem. A* **2001**, *105*, 293−307.

(28) Schmidt, M. W.; Baldridge, K. K.; Boatz, J. A.; Elbert, S. T.; Gordon, M. S.; Jensen, J. H.; Koseki, S.; Matsunaga, N.; Nguyen, K. A.; Su, S. J.; Windus, T. L.; Dupuis, M.; Montgomery, J. A. General Atomic and Molecular Electronic-Structure System. *J. Comput. Chem.* **1993**, *14*, 1347−1363.

(29) Yu, N. T.; Kuck, J. F., Jr.; Askren, C. C. Red fluorescence in older and brunescent human lenses. *Invest. Ophthalmol. Vis. Sci.* **1979**, *18*, 1278−1280.

(30) Kessel, L.; Kalinin, S.; Soroka, V.; Larsen, M.; Johansson, L. B. Impact of UVR-A on whole human lenses, supernatants of buffered human lens homogenates, and purified argpyrimidine and 3-OH-kynurenine. *Acta Ophthalmol. Scand.* **2005**, *83*, 221−227.

(31) Balasubramanian, D. Photodynamics of cataract: an update on endogenous chromophores and antioxidants. *Photochem. Photobiol.* **2005**, *81*, 498−501.

(32) Dillon, J.; Wang, R. H.; Atherton, S. J. Photochemical and photophysical studies on human lens constituents. *Photochem. Photobiol.* **1990**, *52*, 849−854.

(33) Malina, H. Z.; Martin, X. D. Deamination of 3-hydroxykynurenine in bovine lenses: a possible mechanism of cataract formation in general. *Graefes Arch. Clin. Exp. Ophthalmol.* **1995**, *233*, 38−44.